ADVANCED MATERIALS TECHNOLOGIES

Supporting Information

for *Adv. Mater. Technol.*, DOI: 10.1002/admt.202000659

Folding and Bending Planar Coils for Highly Precise Soft Angle Sensing

Hongbo Wang, Massimo Totaro, Selvaraj Veerapandian, Muhammad Ilyas, Minsik Kong, Unyong Jeong, and Lucia Beccai**

WILEY-VCH

Supporting Information

Folding and Bending Planar Coils for Highly Precise Soft Angle Sensing

Hongbo Wang*, Massimo Totaro, Selvaraj Veerapandian, Muhammad Ilyas, Minsik Kong, Unyong Jeong, Lucia Beccai*

Dr. H. Wang, Dr. M. Totaro, Dr. M. Ilyas, Dr. L. Beccai
Center for Micro-BioRobotics, Istituto Italiano di Tecnologia (IIT)
Viale Rinaldo Piaggio 34, Pontedera (Pisa), 56025, Italy

Dr. S. Veerapandian, M. Kong, Prof. U. Jeong
Department of Materials Science and Engineering, Pohang University of Science and Technology
Cheongam-Ro 77, Namgu, Pohang, Gyeongbuk, 37673, Republic of Korea

*Corresponding authors,
Email: Hongbo Wang (hongbo.wang@iit.it), Lucia Beccai (lucia.beccai@iit.it)

Note S1. Theoretical Analysis of Coil Folding

To investigate how the inductance of a planar coil changes when it is folded into two halves, we looked into the simplest case: a single-turn rectangle made of round wire. As illustrated in Figure S1A, trace A'B'CD represents the planar coil, while trace ABQCDP is the coil folded into two equal halves by an angle of β. The length and width of the planar coil are a and b (b=2c), respectively. The diameter of the round wire trace is d_w (radius is r), assuming that it is much smaller than the dimension of the rectangle. It also should be noted that all the calculations below are for low frequency only, which means that the electrical current is evenly spread over the cross-section of the wire (skin effect is negligible). The angle between the two halves of the folded coil is $\theta = \pi - \beta$. Then, the inductance of the flat and folded rectangular coil can be calculated by equations presented in F. W. Gover's book (31), with page number indicated for each cited equation in the text below.

Inductance of a planar rectangular coil

Self-inductance of this rectangular coil can be calculated by (Page 60):

$$L_{rect} = 0.4\left[aln\left(\frac{2a}{r}\right) + bln\left(\frac{2b}{r}\right) + 2\sqrt{a^2+b^2} - asinh^{-1}\left(\frac{a}{b}\right) - bsinh^{-1}\left(\frac{b}{a}\right) - \frac{7}{4}(a+b)\right] \quad \text{(S1)}$$

with a =10 mm, b = 5 mm, and d_w = 0.1 mm, L_{rect} = 26.2698 nH

On another aspect, the inductance of the rectangle is the combination of the self-inductance of these four straight wires and the mutual inductance between them.

$$L_{total} = 2L_{A'B'} + 2L_{B'C} - 2M_{A'B'-CD} - 2M_{B'C-A'D} \quad \text{(S2)}$$

The self-inductance of a straight round wire can be calculated (Page 35):

$$L = 0.2l\left[ln\frac{2l}{r} - \frac{3}{4}\right] \quad \text{(S3)}$$

While, the mutual inductance between two straight round wires is (Page 31):

$$M = 0.2l\left[ln\ ln\left(\frac{l}{d} + \sqrt{1+\frac{l^2}{d^2}}\right) - \sqrt{1+\frac{d^2}{l^2}} + \frac{d}{l}\right] \quad \text{(S4)}$$

Using the same parameter, we can calculate:

$L_{A'B'}$ = 10.4829 nH, $L_{B'C}$ = 4.5483 nH, $M_{A'B'-CD}$ = 1.6512 nH, $M_{B'C-A'D}$ = 0.2451 nH

Then L_{total} = 26.2698 nH, which is exactly the same as direct calculation from Eq. (S1).

Inductance of a folded rectangular coil

When the coil is folded by angle β, the total inductance still can be calculated by the same method by:

$$L_{total} = 2L_{AB} + 2L_{BQC} - 2M_{AB-CD} - 2M_{BQC-APD} \quad \text{(S5)}$$

The self-inductance of the folded trace BQC can be calculated by

$$L_{BQC} = 2L_{BQ} - 2M_{BQ-QC} \tag{S6}$$

Where the mutual inductance between two equal wires (length of *c*) meeting at a point with an angle of θ is (Page 48):

$$M_{BQ-QC} = 0.4c \cdot cos\theta \cdot tanh^{-1}\left(\frac{1}{1+\sqrt{2(1-cos\theta)}}\right) \tag{S7}$$

However, the mutual inductance between two folded wires (BQC-APD) is more complex:

$$M_{BQC-APD} = 2M_{BQ-AP} - 2M_{BQ-PD} \tag{S8}$$

M_{BQ-AP} can be calculated by equation (S4), M_{BQ-PD} can be calculated by (Page 56):

$$M_{BQ-PD} = 0.1cos\theta\left[4c \cdot tanh^{-1}\left(\frac{c}{d_1+d_2}\right) - \Omega\frac{a}{sin\theta}\right] \tag{S9}$$

in which,

$$\Omega = tan^{-1}\left(\frac{a^2cos\theta + c^2sin^2\theta}{ad_1sin\theta}\right) - 2tan^{-1}\left(\frac{a}{d_2tan\theta}\right) + \frac{\pi}{2} - \theta \tag{S10}$$

where d_1 is the distance of BD, and d_2 is the distance of BP, which can be calculated by:

$$\begin{cases} d_1 = \sqrt{a^2 + 2c^2(1-cos\theta)} \\ d_2 = \sqrt{a^2+c^2} \end{cases} \tag{S11}$$

Self and mutual inductances of each part in Eq.(S5), and the total inductance of the folded coil, were calculated and plotted in Figure 1B for a rectangular coil of 10 mm × 5 mm. The curve shows that inductance variation is rather low at small folding angles (98.2% at 45°), and it starts accelerating when the angle is greater than 90°, from 92.1% at 90° down to 78.7% at 135°; then, it drastically decreases to 31.2% at 175°.

In order to validate the results calculated above, a FE model (planar PCB coil model, AD/DC module, COMSOL® Multiphysics) was also created to investigate the inductance changes against different folding angles. The FE model gives an inductance of 28.8244 nH for the same planar rectangular coil (9.7% larger than the theoretical calculation). The difference may be due to the thin-sheet trace used in the FE model, which is different from the round wire assumption used for these equations. As detailed in the next section, numerical analysis was also deployed to calculate the inductance for this single-turn rectangular coil, in order to compare the results from different approaches. As shown in Figure S1B, for the three approaches, the inductance changes have similar trends against the folding angle, with the theoretical analysis resulting in a larger decrease compared to FE modeling, 70.2% and 74.1% at 150°, respectively.

To further investigate the factor of the coil shape, rectangular coils with different length to width ratio (1:2, 1:1, 2:1, and 4:1) were investigated. The results (Figure S1C) indicate that inductance variation is larger for longer coils than for short ones, with inductance decreases to 70.9% and 75.8%

at 150° for the rect-2:1 and 1:2 coils, respectively. Curves of the 4:1 and 2:1 rectangular coils are almost completely overlapped (70.2% vs 70.9% at 150°), indicating that the inductance changes for rectangular coils having a length to width ratio greater than 2:1 do not further increase. It should be acknowledged that eq. (S5) is significantly complex for rectangular coils with more than one turn, making such theoretical analysis impractical.

Note S2. FE Modeling

Simplified 2D FE models were built (using Magnetic fields (mf) study, AC/DC module in COMSOL® Multiphysics) to simulate the cross-section of a long rectangular coil (length is far greater than the width). The coil studied has a width of 10 mm, with 10 turns. The conductive trace has a thickness of 35 µm and a width of 100 µm, with 300 µm space between traces (400 µm pitch). The folding/bending angle controlled geometries of these conductors were created, then a parameter study was performed to calculate the magnetic field for each folding/bending angle (with 0.1 A current as coil excitation), as shown in Figure S2. For the dual-coil case, each coil has a width of 5 mm with only 5 turns, while all other parameters are the same as the single-coil. Finally, the distance between the two coils is 2 mm.

Note S3. Numerical Analysis Methodology

According to Dengler's work (34), the self-inductance of a wire loop can be written as a curve integral akin to the Neumann formula for the mutual inductance of two wire loops:

$$L = \frac{\mu_0}{4\pi}\left[\left(\oint \frac{dX \cdot dX'}{|X - X'|}\right)_{|s-s'|>0.5r} + lY + O\right] \quad \text{(S12)}$$

where $\mu_0 = 4\pi\times10^{-7}$ H/m is the magnetic permeability of vacuum. r denotes the wire radius and l for the total length of the wire. The variable s measures the length along the wire axis. The lY part represents the internal inductance of the wire loop. The constant Y depends on the distribution of the current in the cross-section of the wire: Y = 0 if the current flows in the wire surface, Y = 0.5 when the current is homogeneous across the wire. The ellipse O represents terms like O ($\mu_0 r$) and O ($\mu_0 r/l$), which are negligible for $l >> r$.

Building on Eq. (S12), the inductance of any planar or 3D coil loop can be calculated by dividing the loops into thousands of small segments (filaments), and then performing numerical integration. In this work, MATLAB code was developed for self-inductance calculation of any 3D coil loops by:

$$L = 0.1\left[\sum_{i=1}^{n}\sum_{j=1}^{n}\left(\frac{V_i \cdot V_j}{|S_i - S_j|}\right)_{|S_i-S_j|>0.5r} + 0.5\sum_{i=1}^{n}|V_i|\right] \quad \text{(S13)}$$

where i and j are segments' index of the wire loop, V_i (V_j) is the vector of ith segment, and S_i are the coordinates (x, y, z) of the centre point of the ith segment. The inductance value calculated by Eq. S13 is given in µH. To comprehensively investigate the inductance variations of any planar coil in folded/bent condition, the following steps (Figure S2) have been adopted in the numerical analysis:

I. Creation of coil loop pattern based on the coil shape (circular or rectangular), associated dimensions, number of turns N, and pitches P;

II. Discretization of the coil loops into hundreds to thousands of small segments, with the (x, y) coordinates of all terminals;

III. Coordinate transformation of the planar coil to a folded one, or a bent one. Based on the illustration and equations in Figure 1(D, E, F), 3D coordinates of the folded (x_F, y_F, z_F) or bent (x_B, y_B, z_B) coil at a specific angle can be calculated from 2D coordinates of the original planar coil; IV. With the input of the 3D coordinates of segments representing the 3D coil loop, self-inductance of the folded/bent coil can be calculated by a double layer loop structure in MATLAB (Eq. S13).

Note S4. Electronics for Simultaneous Sensing and Actuation

In Figure 5A, a self-sensorized origami structure was demonstrated by utilizing the flex-coil both to heat the shape memory polymer (SMP) and sense the angle variations of the structure caused by the thermal actuation and/or external stimuli. Ideally, a signal combining the DC part (for heating) and AC signal (for inductance measurement) should be applied to the coil, subsequently the phase and amplitude of the AC current can be analyzed using the AC voltage as reference to obtain the impedance, thereby the resistance and inductance of the coil. In this case study, a simplified method was used to validate the concept by directly connecting a DC current isolation capacitor (C_{ISO}) to block the DC current flow into the LCR meter.

As illustrated in Figure S9A, a 10 μF capacitor (C_{ISO}) was connected in series with the flexible coil, and the DC power supply (including power cables with 1 m length) was connected in parallel with the coil. The LCR meter applied a 2 MHz AC excitation to measure the total impedance (Z_{total}) of the network with the output of an inductance and a resistance connected in series.

$$Z_{total} = R_{total} + j \cdot 2\pi f L_{total} \tag{S14}$$

The power supply and cable can be modeled as a resistor and a capacitor connected in parallel, then with an inductor connected in series, the total impedance is:

$$Z_{PS} = R_{PS} || \left(\frac{1}{2\pi f C_{PS} \cdot j} \right) + j \cdot 2\pi f L_{PS} \tag{S15}$$

From direct measurement at low frequency (1 kHz, $2\pi f L_{PS}$ is negligible) we obtained that: $C_{PS} \approx 200\ \mu F$, $R_{PS} \approx 3\ \Omega$. At f=2 MHz, the capacitance reactance is negligible (0.8 mΩ), then Z_{PS} can be simplified as

$$Z_{PS} \simeq j \cdot 2\pi f L_{PS} \tag{S16}$$

The impedance of the coil can be written as:

$$Z_C = R_C + j \cdot 2\pi f L_C \tag{S17}$$

and capacitive reactance of the C_{ISO} is:

$$X_C = \frac{1}{2\pi f C_{ISO} \cdot j} \tag{S18}$$

where C_{ISO} = 10 μF, we can calculate X_C = -8 mΩ·j, which is negligible. Thus, the main contributions of the total impedance of this network at 2 MHz are the coil and the power supply:

$$\begin{aligned} Z_{total} = Z_C || Z_{PS} &= (R_C + j \cdot 2\pi f L_C) || (j \cdot 2\pi f L_{PS}) \\ &= \frac{4\pi^2 f^2 R_C L_{PS}^2}{R_C^2 + 4\pi^2 f^2 (L_C + L_{PS})^2} + j \cdot 2\pi f L_{PS} \frac{R_C^2 + 4\pi^2 f^2 L_C (L_C + L_{PS})}{R_C^2 + 4\pi^2 f^2 (L_C + L_{PS})^2} \end{aligned} \tag{S19}$$

When the coil is folded by 100°, we measured L_C= 6.78 μH, R_C = 7.93 Ω. Also, direct measurement of the power supply including cable resulted in $L_{PS} \approx 2.80$ μH. Thus, it can be concluded:

$$R_C \ll 4\pi^2 f^2 (L_C + L_{PS})^2 \tag{S20}$$

In this case, the total impedance can be rewritten in a simplified form:

$$Z_{total} = R_C \left(\frac{L_{PS}}{L_C + L_{PS}}\right)^2 + j \cdot 2\pi f \frac{L_C L_{PS}}{L_C + L_{PS}} \tag{S21}$$

Therefore, the total inductance is:

$$L_{total} \simeq \frac{L_C L_{PS}}{L_C + L_{PS}} = L_C \parallel L_{PS} \tag{S22}$$

and the total resistance is:

$$R_{total} \simeq R_C \left(\frac{L_{PS}}{L_C + L_{PS}}\right)^2 \tag{S23}$$

From Eq. (S19) and Eq. (S20), L_{total} (R_{total}) would be significantly smaller than L_C (R_C), as confirmed by the results presented in Figure 5A. Thus, once the total inductance is measured, the coil's inductance can be obtained by

$$L_C \simeq \frac{L_{total} L_{PS}}{L_{PS} - L_{total}} \tag{S24}$$

and the coil's resistance can be obtained by

$$R_c \simeq R_{total} \left(1 + \frac{L_C}{L_{PS}}\right)^2 = R_{total} \left(1 + \frac{L_{total}}{L_{PS} - L_{total}}\right)^2 \tag{S25}$$

However, parasitic parameters (e.g.: cables/wires used to connect these components, energy loss of components at 2 MHz) would contribute to the measured total inductance and resistance (which can be considered as unknown constant values), introducing errors in the calculation of coil's inductance and resistance. Therefore, the total inductance variation measured is:

$$\Delta L_{total} = \frac{L_{PS}(L_{C0} + \Delta L_C)}{L_{PS} + L_{C0} + \Delta L_C} - \frac{L_{PS} L_{C0}}{L_{PS} + L_{C0}} = \frac{L_{PS}^2}{L_{PS} + L_{C0}} \frac{\Delta L_C}{L_{PS} + L_{C0} + \Delta L_C}, \tag{S26}$$

For the origami structure presented in Figure 5A, the coil's inductance is 6.78 μH and 7.45 μH for the pre-deformed shape and remembered shape, respectively. Thus, the total inductance variation can be calculated as 0.054 μH, which is comparable to the experimental results (0.050 μH) shown in Figure 5A. Finally, the coil's inductance variation can be retrieved from the measured total inductance variation and initial inductance values directly:

$$\Delta L_C = \Delta L_{total} \frac{(L_{PS} + L_{C0})^2}{L_{PS}^2 - \Delta L_{total}(L_{PS} + L_{C0})}. \tag{S27}$$

Supporting Figures

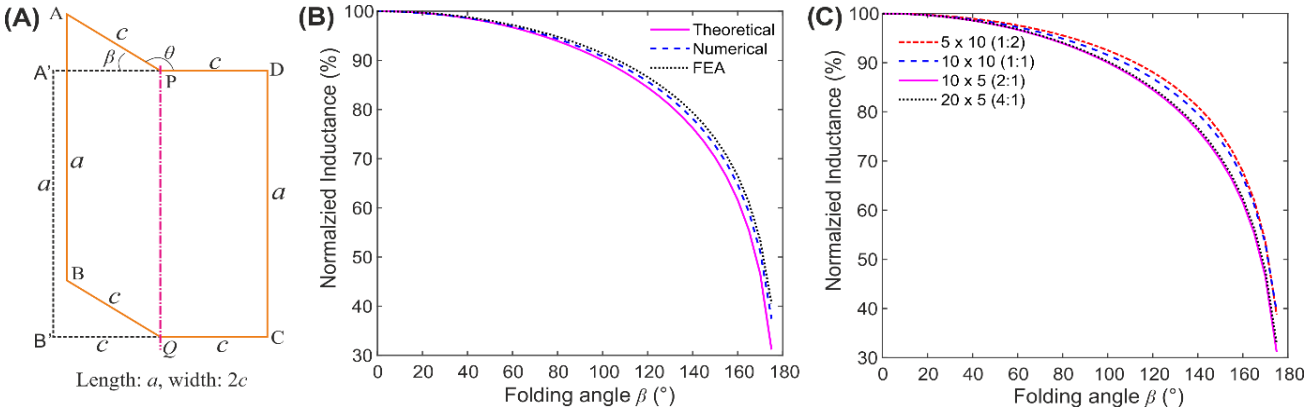

Figure S1. Theoretical analysis of coil folding. (A) Sketch of a single-turn rectangular coil folded into two equal halves; (B) Comparison of inductance calculation from theoretical, numerical, and FE analysis; (C) Theoretical inductance calculation of the folded rectangular coils with different length to width ratios (1:2, 1:1, 2:1, and 4:1).

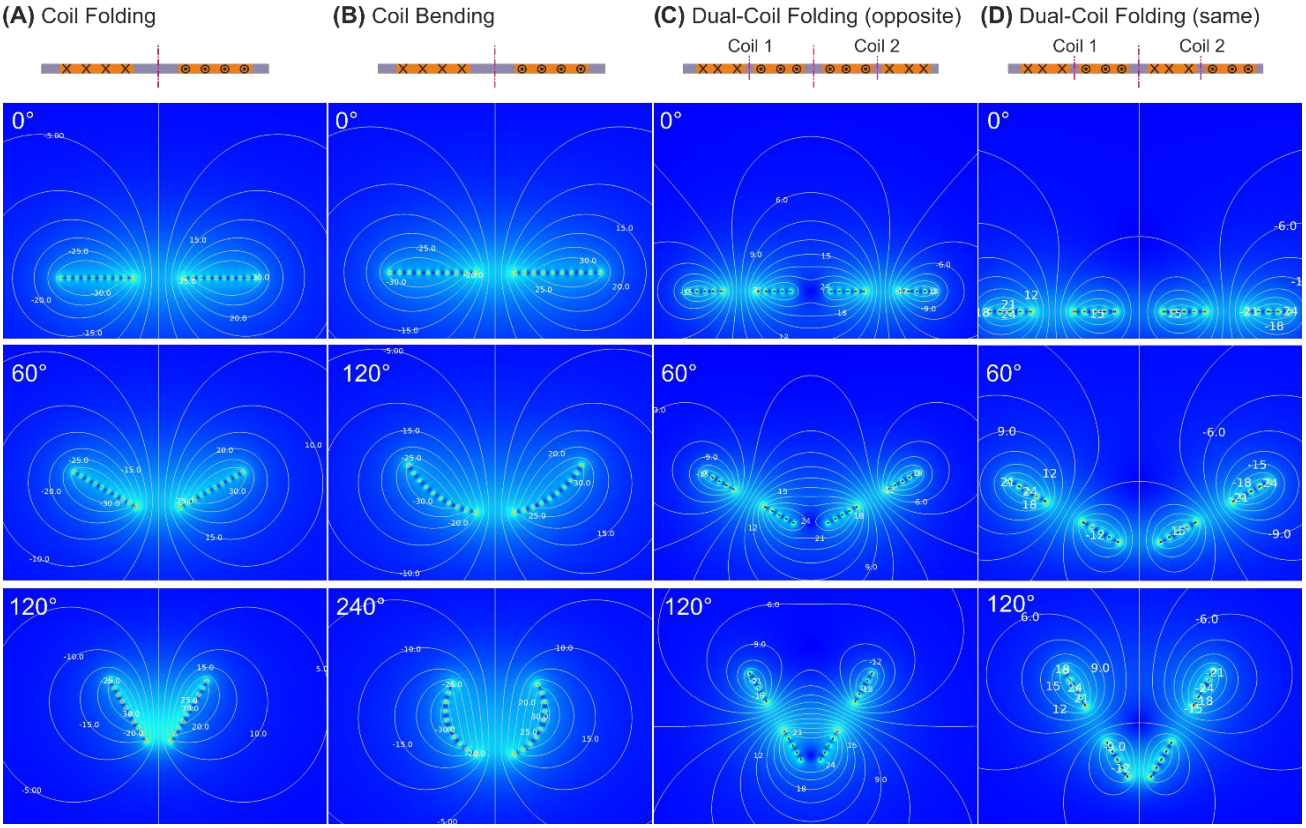

Figure S2. FE modeling of planar coil folding and bending (a cross-section of long rectangular coils). (A) Magnetic field (MF) of a single coil folded at different angles; (B) MF of a single coil bent at different angles/curvatures; (C) MF of a dual-coil with opposite current flow at different folding angles; (D) MF of a dual-coil with same current flow at different folding angles.

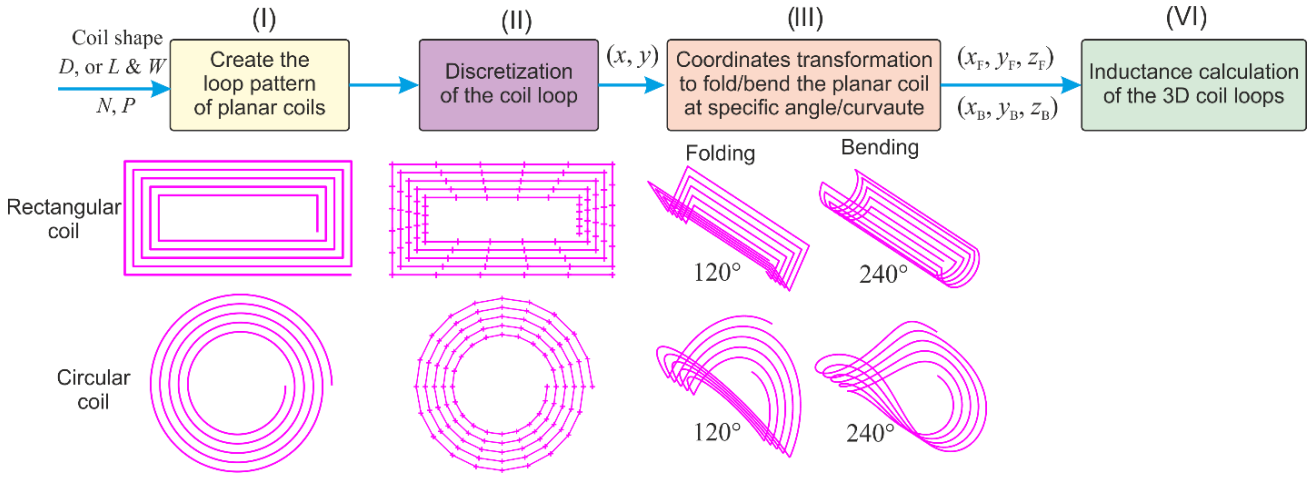

Figure S3. Procedure of the numerical analysis

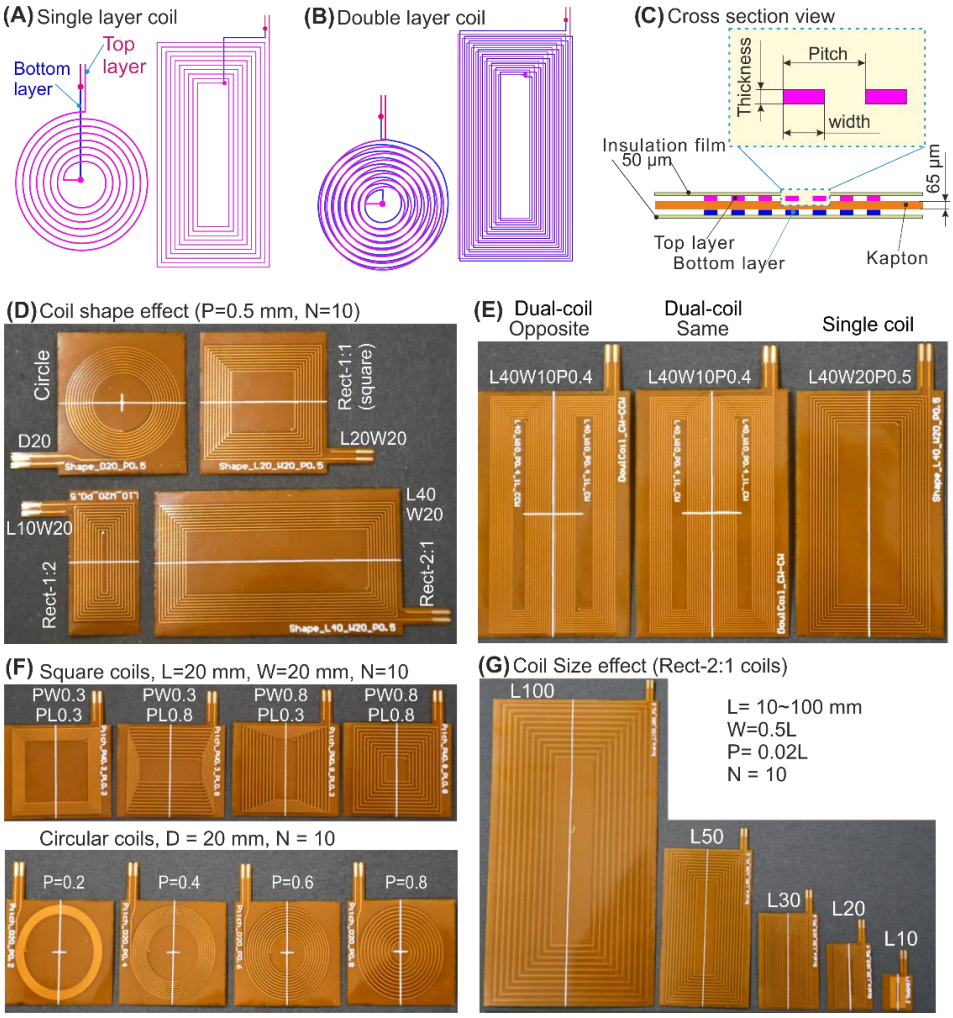

Figure S4. Planar coil design and images of tested FPC coils. (A) Design of single layer coils (circular and rectangle); (B) Design of double layer coils; (C) Cross-section view of double layer FPC coils; (D) Photos of FPC coils with different shapes; (E) Photos of single and dual-coils; (F) Images of coils with the same size but different pitches (square and circular); (G) Rectangular coils with the same design across 10 times scale (100 mm to 10 mm length).

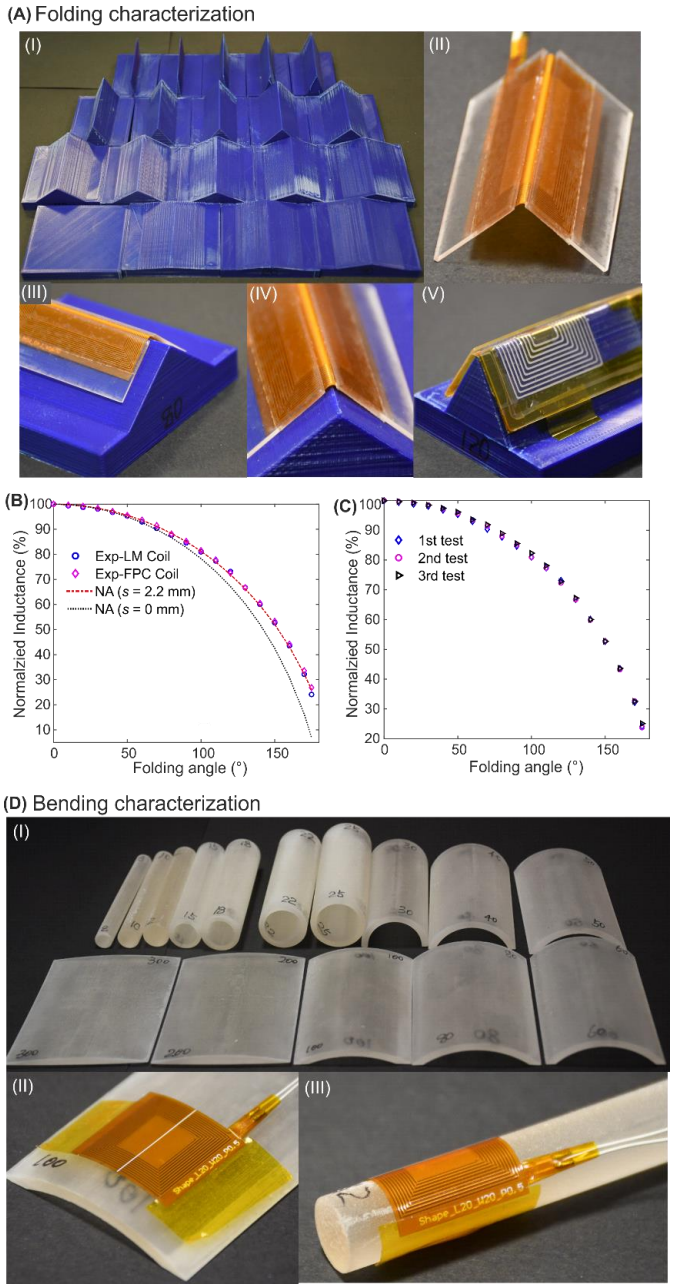

Figure S5. Static characterization methods for coil folding and bending. (A) Folding characterization: (I) Images of 3D printed angle profiles (0° to 175°); (II) Image of a folded FPC coil with two acrylic plates attached; Images of a prepared FPC coil on the 80° angle profile for testing: side view (III) and end view (IV); (V) Image of a LM coil on the 120° angle profile for testing; (B) Inductance variation comparison of folded LM and FPC coils with the same design; (C) Results of repeated folding tests of the same coil. (D) Bending characterization: (I) Images of 3D printed curvature profiles (rods, tubes and cylindrical surfaces with diameters from 8 mm to 300 mm); (II) Image of a square FPC coil on a 100 mm diameter cylinder surface; (III) Image of a square FPC coil wrapped on a rod with a diameter of 12 mm.

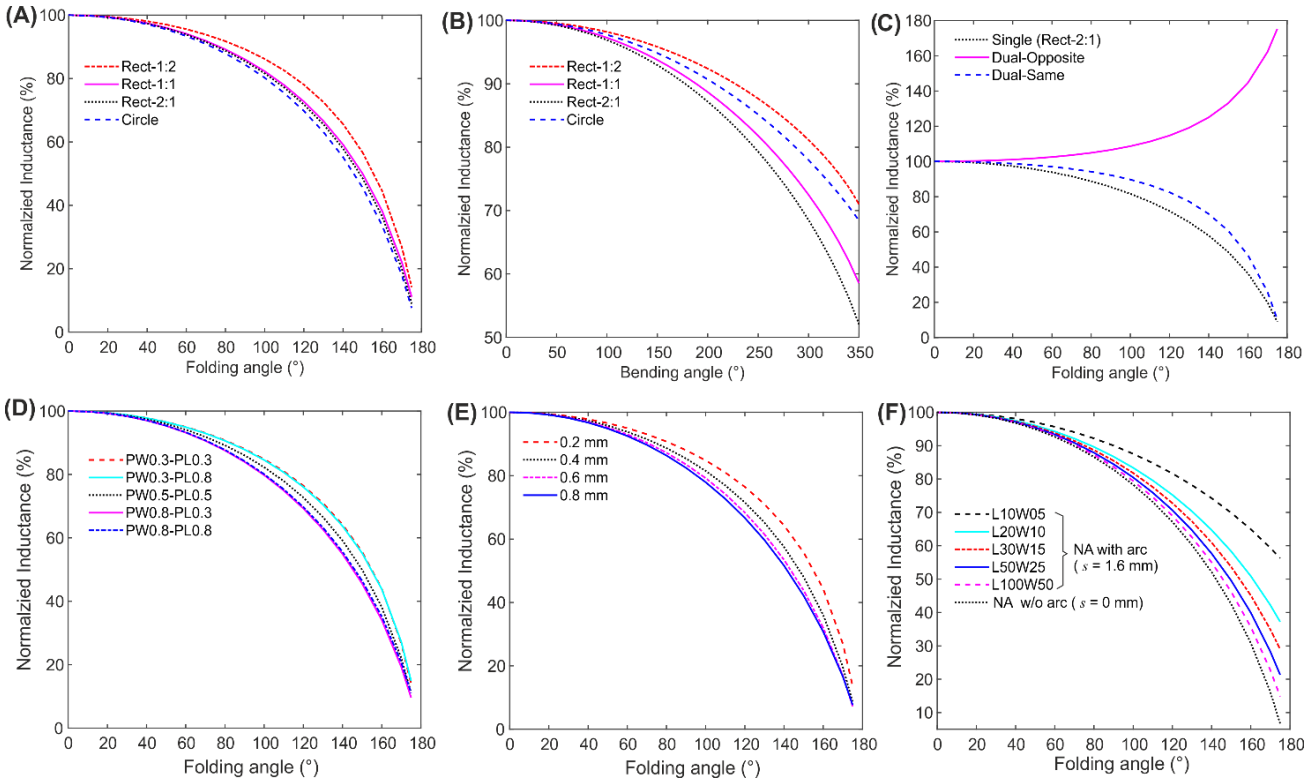

Figure S6. Numerical analysis results of planar coils with different design parameters. (A) Folding of coils with different shapes; (B) Bending of coils with different shapes; (C) Folding of single and dual-coils with opposite/same current directions; (D) Folding of rectangular coils with different pitches; (E) Folding of circular coils with different pitches; (F) Folding with a 1.6 mm arc of rectangular coils with different sizes.

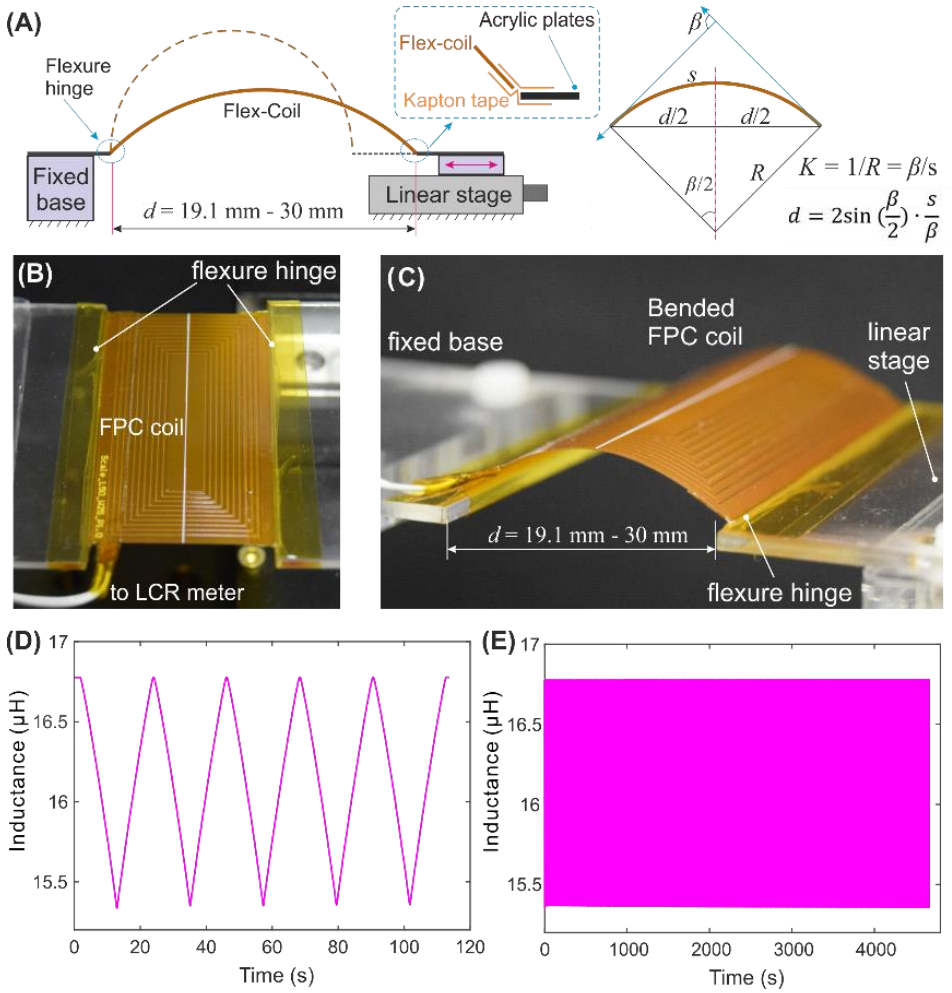

Figure S7. Dynamic bending experiments setup and cyclic testing results. (A) Sketch of the FPC coil bending test setup; (B) Image of a FPC coil at flat state (top view); (C) Image of a FPC coil at bended state (perspective view); (D) Inductance variations of 5 bending-releasing cycles; (E) Inductance variations of 1000 bending-releasing cycles (5 mm/s).

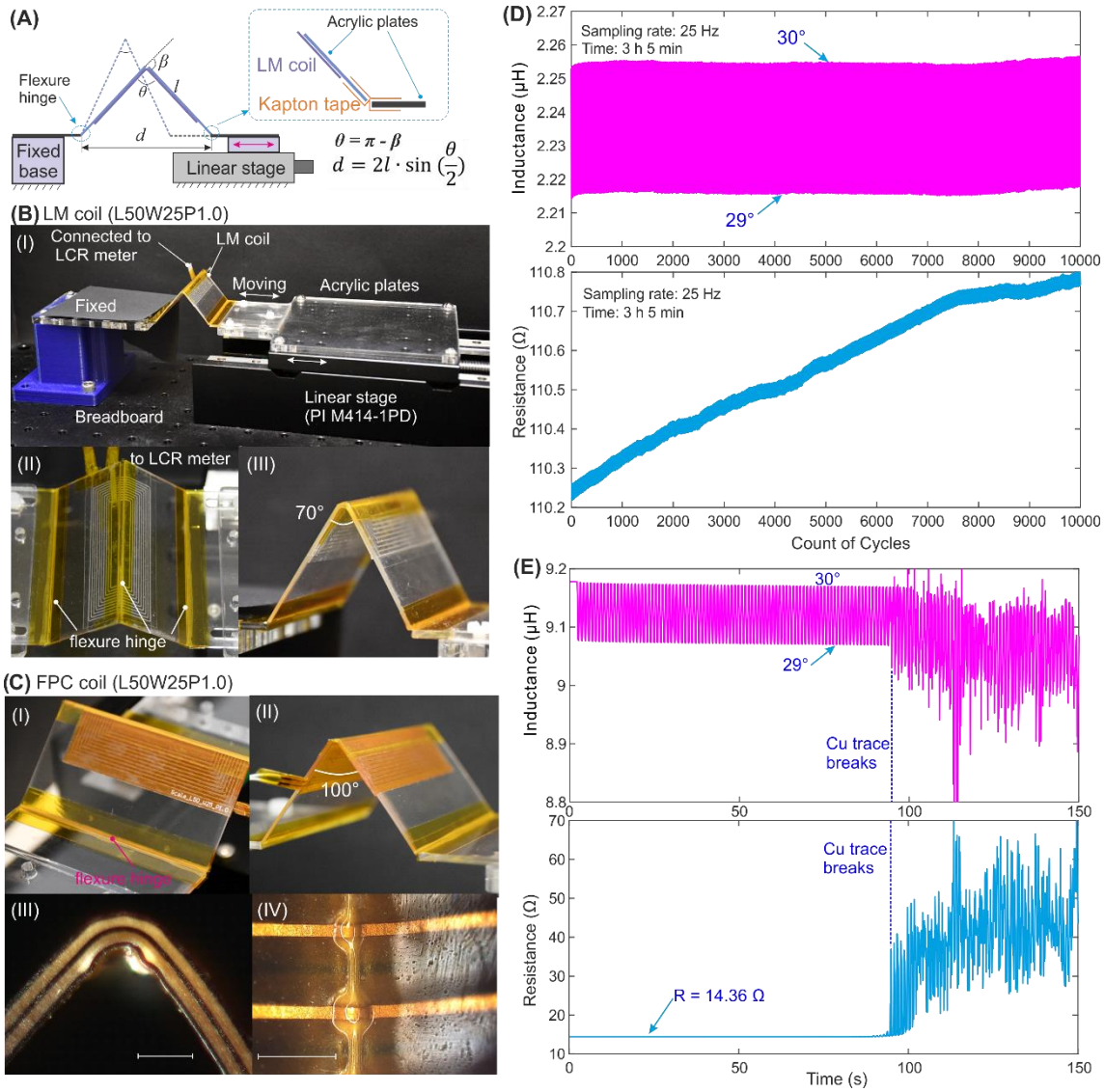

Figure S8. Dynamic folding experiments setup and cyclic testing results. (A) Sketch of the FPC coil folding test setup; (B) Images of LM coils folding tests: (I) the whole experimental setup; (II) top view of the folded LM coil; (III) side view of the LM coil; (C) Images of folded FPC coils: (I) top-side view; (II) side view; (III) magnified image of the folded double layer FPC coil (side); (IV) magnified image to show the delamination of a FPC coil after hundreds of repeated folding cycles (29°-30°); (D) Inductance and resistance variations of a LM coil during a 10000 cycles of 1° folding-unfolding (29°-30°); (E) Inductance and resistance variations of a FPC coil before and after the copper trace breaks under a cyclic 1° folding-unfolding test.

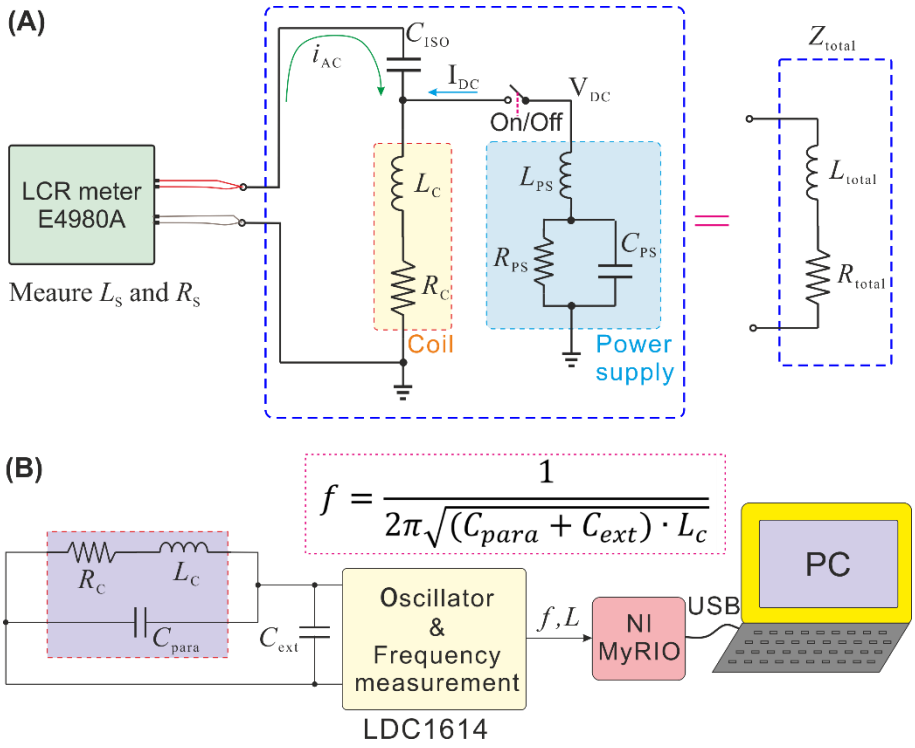

Figure S9. Electronic circuits of inductance measurement systems. (A) Electronic circuits to simultaneously measure the inductance and to heat the coil; (B) LC oscillator-based electronic system with high sampling rate inductance measurement (500 Hz) for vibration detection.

Supporting Tables

Table S1. List of all planar coils and their parameters

Coil	"Label"	Length (mm)	Width (mm)	Pitch (length)	Pitch (width)	*L* (μH)	*R* (Ω)	Notes
FPC coils-Rectangle	L10W20P0.5	10	20	0.5	0.5	5.0572	5.3662	
	L20W20P0.5	20	20	0.5	0.5	10.133	7.5742	
	L40W20P0.5	40	20	0.5	0.5	18.876	12.607	
	L20W20PL0.3PW0.3	20	20	0.3	0.3	14.336	8.5621	
	L20W20PL0.8PW0.3	20	20	0.8	0.3	9.3259	7.2001	
	L20W20PL0.3PW0.8	20	20	0.3	0.8	9.1121	7.1921	
	L20W20PL0.8PW0.8	20	20	0.8	0.8	6.2141	6.3885	
	L10W05P0.2	10	5	0.2	0.2	3.2162	2.7214	
	L20W10P0.4	20	10	0.4	0.4	6.4217	5.4932	
	L30W15P0.6	30	15	0.6	0.6	9.6314	8.2832	
	L50W25P1.0	50	25	1.0	1.0	16.177	14.428	
	L75W16P0.5	75	16	0.5	0.5	28.636	12.385	
	L100W50P2.0	100	50	2.0	2.0	32.421	28.283	
LM Coils-Rectangle	L50W25P1.0	50	25	1.0	1.0	4.2754	124.55	1 layer
	L30W30P1.2	30	30	1.2	1.2	2.5612	63.052	1 layer
FPC Coils Dual-rectangle	DualCoil_CW-CW	40	10	0.4	0.4	6.3053	9.5591	1 layer
	DualCoil_CW-CCW	40	10	0.4	0.4	7.4144	10.228	1 layer
Coils	"Label"	Diameter (mm)		Pitch (mm)		L	R	Notes
FPC coils-Circle	D20P0.5	20		0.5		8.0336	6.0684	
	D20P0.2	20		0.2		14.008	6.2607	
	D20P0.4	20		0.4		9.5799	5.8545	
	D20P0.6	20		0.6		6.7464	5.5201	
	D20P0.8	20		0.8		4.7376	4.5128	
	D5P0.2	5		0.2		1.3524	1.2862	
	D10P0.4	10		0.4		2.4789	2.4188	
	D30P1.2	30		1.2		7.0425	6.7703	
	D50P2.0	50		2.0		11.808	11.881	

Note 1: All coils have 10 turns per layer, and 2 layers except for these marked as 1 layer.
Note 2: All the inductance and resistance were measured with a LCR meter (Agilent E4980A) at 200 kHz. A pair of short leading wires were used between the coils and LCR meter probes, which contributes to an inductance value of 0.3722 μH, and resistance of 0.2876 Ω (in average) to the *L* and *R* values listed in this table.

Supporting Movies (.MP4 format)

Movie S1. FE modeling of planar coil folding and bending

Movie S2. Numerical analysis of planar coil folding and bending

Movie S3. Dynamic bending test of FPC coil

Movie S4. Dynamic folding test of LM coil

Movie S5. Vibration detection with a folded FPC coil

Movie S6. Self-sensing origami

Movie S7. Sensorized soft pneumatic actuator

Movie S8. Wearable sensing